IEICE TRANS. COMMUN., VOL.E92–B, NO.10 OCTOBER 2009

PAPER

A New User Selection Measure in Block Diagonalization Algorithm for Multiuser MIMO Systems

Riichi KUDO[†a)], **Yasushi TAKATORI**[†], **Kentaro NISHIMORI**[†], **Atsushi OHTA**[†], **Shuji KUBOTA**[††], *and* **Masato MIZOGUCHI**[†], *Members*

SUMMARY Multiuser — Multiple Input Multiple Output (MU-MIMO) techniques were proposed to increase spectrum efficiency; a key assumption was that the Mobile Terminals (MTs) were simple with only a few antennas. This paper focuses on the Block Diagonalization algorithm (BD) based on the equal power allocation strategy as a practical MU-MIMO technique. When there are many MTs inside the service area of the access point (AP), the AP must determine, at each time slot, the subset of the MTs to be spatially multiplexed. Since the transmission performance depends on the subsets of MTs, the user selection method needs to use the Channel State Information (CSI) obtained in the physical layer to maximize the Achievable Transmission Rate (ATR). In this paper, we clarify the relationship between ATR with SU-MIMO and that with MU-MIMO in a high eigenvalue channel. Based on the derived relationship, we propose a new measure for user selection. The new measure, the eigenvalue decay factor, represents the degradation of the eigenvalues in null space compared to those in SU-MIMO; it is obtained from the signal space vectors of the MTs. A user selection method based on the proposed measure identifies the combination of MTs that yields the highest ATR; our approach also reduces the computational load of user selection. We evaluate the effectiveness of user selection with the new measure using numerical formulations and computer simulations.

key words: *multiuser MIMO, user selection, block diagonalization, channel capacity*

1. Introduction

Multiple Input Multiple Output (MIMO) systems promise higher spectrum utilization in multipath-rich environments [1], [2]. The capacity gain roughly increases in proportion to the minimum number of receive and transmit antennas, but the number of antennas at a Mobile Terminal (MT) is restricted because of cost and size limitations. The Access Point (AP), on the other hand, can possess a larger number of antennas. The small number of antennas at the MT limits the improvement in capacity.

One technique that further improves the spectrum utilization is MUltiuser (MU)-MIMO [3]. MU-MIMO systems are expected to offer a larger spatial diversity effect than Single User (SU) -MIMO. Dirty Paper Coding (DPC) [4] is a well known coding scheme that achieves the maximum sum capacity [5]. Although DPC is optimal for downlink MU-MIMO, it is impractical to implement due to its extremely high computational load. The Block Diagonalization (BD) algorithm was proposed as a practical linear precoding technique for MU-MIMO systems [6]–[10]. In BD, signals are transmitted to an MT so as not to interfere with the other MTs. The Achievable Transmission Rate (ATR) with BD is inferior to that with DPC since the former limits the signal space to the null space of all other MT's channels while the latter allows the signal spaces to overlap. However, it has been shown that ATR with BD approaches the performance of DPC as the number of users increases [3], [11].

When there are many MTs inside the service area of the AP, the AP must, due to the limited dimensionality of the signal space, determine a subset of MTs that the AP will communicate with simultaneously [12]. The transmission performance in MU-MIMO depends on the subset of MTs selected. Furthermore, we consider that the AP must eventually communicate all the MTs to meet the fairness requirement. Since the number of MT combinations possible explodes, the AP cannot estimate the transmission performances corresponding to all possible MT subsets. To determine the subset of MTs with practical computational load, user selection methods that employ CSI were proposed for the scenario wherein each MT has a single receive antenna branch [13]–[16]. User selection methods for MTs with more than two receive antennas have also been proposed [17]–[20]. The user selection methods in [17]–[19] utilize the capacity or norm of the channel in the null space of all other MTs in the subset as the selection measure.

The user selection methods based on capacity or norm of the channel attain high ATR if we can assume that all MTs have the same Signal to Noise Ratios (SNRs) among MTs. This is because the channel capacity and channel norm in MU-MIMO are directly related to the correlation between the MTs' signal spaces. When SNRs of the MTs vary widely, high SNR MTs are chosen first and remaining low SNR MTs degrade the overall ATR.

A user selection method that utilizes another measure was proposed in [20]; it selects the MTs subset that minimizes the correlation between the MT subspaces. [20] showed that user selection methods based on correlation and capacity have almost the same performance if all MTs have the same SNR. When there are SNR variations among the active MTs, it is expected that correlation-based methods will be superior to user selection based on capacity. However, the relationship between correlation of the MT subspaces and the ATR with BD is not clearly identified in [20].

This paper proposes a new measure for user selection

Manuscript received June 1, 2009.

[†]The authors are with NTT Network Innovation Laboratories, NTT Corporation, Yokosuka-shi, 239-0847 Japan.

[††]The author is with Shibaura Institute of Technology, Tokyo, 135-8548 Japan.

a) E-mail: kudo.riichi@lab.ntt.co.jp

DOI: 10.1587/transcom.E92.B.3206

that avoids the above problems. The new measure, the eigenvalue decay factor, is derived from the signal spaces of the MTs subset. The eigenvalue decay factor clarifies the relationship between the ATR with BD and the spatial separability of MTs [21]; this measure has lower computational load than conventional user selection schemes. Since a user selection method based on the measure utilizes the base vectors corresponding to the signal spaces of the MTs subset, its performance is not influenced by SNR variation. A user selection method with the new measure is subjected to simulations assuming an environment wherein there are SNR variations.

In this paper, we assume that the transmitter allocates equal power to all users to better show the basic characteristics of the new user selection measure. Although equal power allocation does not maximize the overall throughput, the investigation of the performance with equal power allocation is still valuable because of its simplicity as explained in [22]. The reduction in calculation overhead for the large number of MT case is one of the most important issues addressed by this paper.

This paper is organized as follows. Section 2 describes BD transmission in the MU-MIMO system and EigenVector transmission (EV) in the SU-MIMO system. In Sect. 3, we analytically investigate the ATR and derive a simplified expression that clarifies the relationship between the ATR with MU-MIMO and the signal spaces for the MTs subset. Based on the derived expression, a new measure is proposed for user selection. Section 4 presents user selection methods based on the new measure as well as the conventional methods based on the capacity and norm of the channel. A comparison of their computational loads is also presented. Section 5 introduces a simulation that examines ATR with user selection based on the proposed and conventional measures. Finally, Section 6 summarizes the paper.

Throughout the paper, superscript *, superscript H, and $\|.\|_F$ denote the complex conjugate, the Hermitian transposition, and the Frobenius norm, respectively. Term $|\mathbf{A}|$ is the determinant of $\mathbf{A}$.

2. Transmission Method

The downlink transmission of a narrowband MU-MIMO system is considered. The number of active MTs is assumed to be K. The AP and each MT have N transmit antennas and M receive antennas, respectively. The AP communicates with all selected MTs via L time slots. In each time slot, the AP communicates with U MTs. Thus, K is expressed as $U \times L$. The total number of receive antennas at the supported MTs in the same time slot is assumed to be less than or equal to the number of transmit antennas. This means that $U \times M \leq N$. The CSI between the AP and MT k, is represented by the channel matrix $\mathbf{H}_k \in \mathbb{C}^{M \times N}$. It is assumed that the AP and MT k share CSI perfectly.

Signal $\mathbf{y}_k$ received by MT k in the l-th time slot is represented as

$$\mathbf{y}_k = \mathbf{H}_k \sum_{i=1}^{U} \mathbf{W}_{\phi_l(i)} \mathbf{P}_{\phi_l(i)} \mathbf{x}_{\phi_l(i)} + \mathbf{n}_k, \tag{1}$$

where $\mathbf{P}_i \in \mathbb{C}^{M \times M}$, $\mathbf{x}_i \in \mathbb{C}^{M \times 1}$, and $\mathbf{W}_i \in \mathbb{C}^{N \times M}$ are the power allocation matrix, the transmitted signal, and the transmission weight, respectively. $\phi_l(i)$ denotes the i-th MT in the l-th time slot. The power allocation matrix for MT k, $\mathbf{P}_k$, is a diagonal matrix whose diagonal elements are expressed as square roots of power allocation elements, $p_{k,1}, \ldots, p_{k,Mk}$ as follows.

$$\mathbf{P}_k = \begin{pmatrix} \sqrt{p_{k,1}} & 0 & \cdots & 0 \\ 0 & \sqrt{p_{k,2}} & & \vdots \\ \vdots & & \ddots & 0 \\ 0 & \cdots & 0 & \sqrt{p_{k,M}} \end{pmatrix}, \tag{2}$$

where $\mathbf{n}_k$ is the noise vector of MT k. The elements of the noise vector are assumed to have a variance of one.

The expectation and covariance values of the element of the transmitted signal, $\mathbf{x}_i$, are defined to be zero and one, respectively. We denote the subset of MTs selected in the l-th time slot as $\{\Phi_l = \phi_l(1), \ldots, \phi_l(U)\}$ and the combinations of all subsets as $\{\Psi = \Phi_1, \ldots, \Phi_L\}$. K MTs are included in Ψ and overlapping is not allowed. Thus, $\phi_l(i) \neq \phi_m(j)$ where $l \neq m$. In (1), MT k is included in Φ_l and $k = \phi_l(\kappa)$. The transmission power, P, is obtained as $\sum_{k \in \Phi_l} \left\| \mathbf{P}_{\Phi_l,k} \right\|_F^2$. Since we assume equal power allocation among users, the transmission power for MT $\phi_l(\kappa)$ is denoted as P/U.

2.1 Block Diagonalization

The BD algorithm utilizes the null space of the other MTs in the subset to ensure that the signals transmitted to MT k do not interfere with those to the other MTs. To simplify the following explanation, we focus on the l-th time slot and omit the time slot subscript. Thus, we define the subset of MTs selected in the l-th time slot as $\Phi_l = \Phi = \{\phi(1), \ldots, \phi(U)\}$. The aggregate channel matrix for MT k, $\tilde{\mathbf{H}}_{\Phi,k}$, is defined as $\left(\mathbf{H}_{\phi(1)}^T \cdots \mathbf{H}_{\phi(\kappa-1)}^T \mathbf{H}_{\phi(\kappa+1)}^T \cdots \mathbf{H}_{\phi(U_l)}^T\right)^T \in \mathbb{C}^{(U-1)M \times N}$, where $\Phi = \{\phi(1), \cdots \phi(\kappa) = k, \cdots \phi(U)\}$. $\tilde{\mathbf{H}}_{\Phi,k}$ is subjected to Singular Value Decomposition (SVD) as follows

$$\tilde{\mathbf{H}}_{\Phi,k} = \tilde{\mathbf{U}}_{\Phi,k} \begin{pmatrix} \tilde{\mathbf{\Sigma}}_{\Phi,k} & \mathbf{0} \end{pmatrix} \begin{pmatrix} \tilde{\mathbf{V}}_{\Phi,k}^{(s)} & \tilde{\mathbf{V}}_{\Phi,k}^{(n)} \end{pmatrix}^H, \tag{3}$$

where $\tilde{\mathbf{V}}_{\Phi,k}^{(s)} \in \mathbb{C}^{N \times (U-1)M}$ represents the signal space of all MTs except for MT k and $\tilde{\mathbf{V}}_{\Phi,k}^{(n)} \in \mathbb{C}^{N \times (N-(U-1)M)}$ represents the null space that does not interfere with the other MTs in subset Φ. $\tilde{\mathbf{U}}_{\Phi,k} \in \mathbb{C}^{(U-1)M \times (U-1)M}$ is the left singular vectors. SVD is then performed on the null space channel matrix, $\mathbf{H}_k \tilde{\mathbf{V}}_{\Phi,k}^{(n)}$, as

$$\mathbf{H}_k \tilde{\mathbf{V}}_{\Phi,k}^{(n)} = \bar{\mathbf{U}}_{\Phi,k} \bar{\mathbf{\Sigma}}_{\Phi,k} \bar{\mathbf{V}}_{\Phi,k}^{(s)H}, \tag{4}$$

where $\bar{\mathbf{\Sigma}}_{\Phi,k} \in \mathbb{C}^{M \times M}$ is the diagonal matrix and the diagonal

elements of $\bar{\mathbf{\Sigma}}_{\Phi,k}$ are the square roots of the null space eigenvalues, $\bar{\lambda}_{\Phi,k,1}, \bar{\lambda}_{\Phi,k,2}, \cdots, \bar{\lambda}_{\Phi,k,M}$, which are the eigenvalues of $\mathbf{H}_k \tilde{\mathbf{V}}^{(n)}_{\Phi,k} \tilde{\mathbf{V}}^{(n)H}_{\Phi,k} \mathbf{H}^H_k$. $\bar{\mathbf{U}}_{\Phi,k}$ and $\bar{\mathbf{V}}^{(s)}_{\Phi,k}$ are the left and right singular vectors, respectively. The transmission weight matrix for MT k, $\bar{\mathbf{W}}_{\Phi,k}$, is given as $\tilde{\mathbf{V}}^{(n)}_{\Phi,k} \bar{\mathbf{V}}^{(s)}_{\Phi,k}$ and the transmission qualities of the data streams correspond to the diagonal elements of $\bar{\mathbf{\Sigma}}_{\Phi,k}$. Since $\mathbf{H}_j \bar{\mathbf{W}}_{\Phi,i} = \mathbf{0}$ where $i \neq j$, the signal received by MT k can be rewritten as

$$\begin{aligned}\mathbf{y}_k &= \mathbf{H}_k \sum_{i=1}^{U} \bar{\mathbf{W}}_{\Phi,i} \mathbf{P}_{\Phi,i} \mathbf{x}_i + \mathbf{n}_k \\ &= \mathbf{H}_k \bar{\mathbf{W}}_{\Phi,k} \mathbf{P}_{\Phi,k} \mathbf{x}_k + \mathbf{n}_k. \end{aligned} \tag{5}$$

The ATR for MT k in the l-th subset Φ_l with BD is given as

$$\begin{aligned} C_{MU,\Phi_l,k} &= T_{MU} \log_2 \left| \mathbf{I}_M + \mathbf{H}_k \tilde{\mathbf{V}}^{(n)}_{\Phi_l,k} \bar{\mathbf{V}}^{(s)}_{\Phi_l,k} \mathbf{P}^2_{\Phi_l,k} \bar{\mathbf{V}}^{(s)H}_{\Phi_l,k} \tilde{\mathbf{V}}^{(n)H}_{\Phi_l,k} \mathbf{H}^H_k \right| \\ &= T_{MU} \log_2 \Big| \mathbf{I}_M + \bar{\mathbf{U}}_{\Phi_l,k} \bar{\mathbf{\Sigma}}_{\Phi_l,k} \bar{\mathbf{V}}^{(s)H}_{\Phi_l,k} \bar{\mathbf{V}}^{(s)}_{\Phi_l,k} \\ &\qquad \mathbf{P}^2_{\Phi_l,k} \bar{\mathbf{V}}^{(s)H}_{\Phi_l,k} \bar{\mathbf{V}}^{(s)}_{\Phi_l,k} \bar{\mathbf{\Sigma}}_{\Phi_l,k} \bar{\mathbf{U}}^H_{\Phi_l,k} \Big| \\ &= T_{MU} \log_2 \left| \mathbf{I}_M + \bar{\mathbf{\Sigma}}^2_{\Phi_l,k} \mathbf{P}^2_{\Phi_l,k} \right| \\ &= T_{MU} \sum_{i=1}^{M} \log_2 \left(1 + p_{\Phi_l,k,i} \bar{\lambda}_{\Phi_l,k,i}\right). \end{aligned} \tag{6}$$

Since the variance of the noise is assumed to be one, SNR is obtained using the power allocation elements and eigenvalues. To define the sum rate, which is the channel capacity corresponding to all MTs, T_{MU} is used as the normalized time duration. We assume that the summation of the normalized time duration is one and T_{MU} is expressed as $1/L$. Although this equal power allocation assumption does not maximize the sum rate for all MTs, all MTs can have an opportunity to improve their ATR compared to SU-MIMO. The total ATR in the l-th time slot, C_{MU,Φ_l}, and the sum rate for all subsets $\Psi = \{\Phi_1, \Phi_2, \cdots \Phi_L\}$, C_{MU}, are expressed as

$$C_{MU,\Phi_l} = \sum_{i \in \Phi_l} C_{MU,\Phi_l,i}, \tag{7}$$

$$C_{MU} = \sum_{l=1}^{L} \sum_{i \in \Phi_l} C_{MU,\Phi_l,i}. \tag{8}$$

To estimate the ATR with BD, the AP must calculate $\tilde{\mathbf{V}}^{(n)}_{\Phi_l,k}$ and the null space channel matrix, $\mathbf{H}_k \tilde{\mathbf{V}}^{(n)}_{\Phi_l,k}$, of all subsets. The complexity of this calculation overwhelms the AP.

2.2 Eigenvector Transmission

To investigate the ATR improvement in MU-MIMO, we examine ATR with SU-MIMO in a TDMA system. In this paper, EigenVector transmission (EV) is used as the SU-MIMO transmission technique. By using SVD, the channel matrix for MT k is expressed as

$$\mathbf{H}_k = \mathbf{U}_k \begin{pmatrix} \mathbf{\Sigma}_k & \mathbf{0} \end{pmatrix} \begin{pmatrix} \mathbf{V}^{(s)}_k & \mathbf{V}^{(n)}_k \end{pmatrix}^H, \tag{9}$$

where $\mathbf{V}^{(s)}_k \in \mathbb{C}^{N \times M}$ and $\mathbf{V}^{(n)}_k \in \mathbb{C}^{N \times (N-M)}$ represent the right singular vectors for the signal space and the null space, respectively. The diagonal elements of Σ_k are the square roots of $\lambda_{k,1}, \lambda_{k,2}, \cdots \lambda_{k,M}$, which are the eigenvalues of $\mathbf{H}^H_k \mathbf{H}_k$. The ATR with EV is expressed as

$$\begin{aligned} C_{SU,k} &= T_{SU} \log_2 \left| \mathbf{I}_{M_k} + \mathbf{H}_k \mathbf{V}^{(s)}_k \mathbf{P}^2_k \mathbf{V}^{(s)H}_k \mathbf{H}^H_k \right| \\ &= T_{SU} \sum_{i=1}^{M_k} \log_2 \left(1 + p_{k,i} \lambda_{k,i}\right), \end{aligned} \tag{10}$$

where T_{SU} is the normalized time duration in EV; its summation is assumed to be one. Since the same time duration is assumed to be allocated to each MT, T_{SU} is expressed as $1/K$. $\mathbf{P}_k$ is the power allocation matrix for EV and $\|\mathbf{P}_k\|^2_F = P$. The power allocation elements are decided using the water filling strategy [23] with the eigenvalues, $\lambda_{k,1}, \lambda_{k,2}, \cdots \lambda_{k,Mk}$. Thus, the sum rate with EV is expressed as

$$C_{SU} = \sum_{i=1}^{K} C_{SU,i}. \tag{11}$$

To compare the total ATR with BD corresponding to the l-th subset Φ_l in (7), the total ATR with EV corresponding to Φ_l is defined as

$$C_{SU,\Phi_l} = \sum_{i \in \Phi_l} C_{SU,i}. \tag{12}$$

3. Eigenvalue Decay Factor for User Selection Method

First, we introduce the eigenvalue decay factors that express the relationship between the null space eigenvalues in BD and the original eigenvalues, i.e. the eigenvalues in SU-MIMO, as in

$$\bar{\lambda}_{\Phi,k,i} = a_{\Phi,k,i} \lambda_{k,i}, \tag{13}$$

where $a_{\Phi,k,i}$ is the eigenvalue decay factor. The region of the decay factor is given as

$$0 \leq a_{\Phi,k,i} \leq 1. \tag{14}$$

A detailed derivation of the above inequality is presented in Appendix. The decay factor expresses the degradation of the transmission space when using BD. The new measure is the key to more effective user selection for BD. In this section, we show the relationship between the ATR with BD and the decay factor.

3.1 Relationship between ATRs in BD and EV

Here, we focus on the high SNR scenario. In this scenario, the effectiveness of MU-MIMO is large [6], [7], and the following inequality is expected to be satisfied.

$$1 \ll \bar{\lambda}_{\Phi,k,i} \leq \lambda_{k,i}; \tag{15}$$

the variance of the noise is omitted since that is assumed to

be one. In high SNR and multipath-rich environments, the contribution of the water filling strategy becomes negligible [24] and the optimum power allocation among data streams approaches equal power allocation. Thus, the power allocation elements for BD and EV are approximated as $p_{\Phi_l,k,1} \approx \cdots \approx p_{\Phi_l,k,M} \approx P/(MU)$ and $p_{s,k,1} \approx \cdots \approx p_{s,k,M} \approx P/M$, respectively. The ATR in MU-MIMO, $C_{MU,\Phi l,k}$, in (6) and that in SU-MIMO, $C_{SU,k}$, in (10) are approximated as

$$C_{MU,\Phi_l,k} \approx T_{MU} \sum_{i=1}^{M} \log_2\left(\frac{P\bar{\lambda}_{\Phi_l,k,i}}{UM}\right) \tag{16}$$

$$C_{SU,k} \approx T_{SU} \sum_{i=1}^{M} \log_2\left(\frac{P\lambda_{k,i}}{M}\right). \tag{17}$$

Therefore, $C_{MU,\Phi_l,k}$, is rewritten as

$$\begin{aligned} C_{MU,\Phi_l,k} &\approx T_{MU} \sum_{i=1}^{M_k} \log_2\left(\frac{P\bar{\lambda}_{\Phi_l,k,i}}{UM}\right) \\ &= T_{MU}\left(\sum_{i=1}^{M} \log_2\left(\frac{P\lambda_{k,i}}{M}\right)\right. \\ &\quad \left. + \sum_{i=1}^{M} \log_2\left(\frac{a_{\Phi_l,k,i}}{U}\right)\right) \\ &= \frac{T_{MU}}{T_{SU}} C_{SU,k} - T_{MU} M \log_2 U \\ &\quad + T_{MU} \log_2 \Lambda_{\Phi_l,k}, \end{aligned} \tag{18}$$

where $\Lambda_{\Phi_l,k}$ is the decay factor product expressed as

$$\Lambda_{\Phi_l,k} = \prod_{i=1}^{M} a_{\Phi_l,k,i}. \tag{19}$$

We will discuss the characteristics of the decay factor in the next subsection. Since multiple MTs communicate with the AP simultaneously, the time duration for BD, T_{MU}, is larger than that for SU-MIMO, T_{SU}. Therefore, the improvement in ATR with BD compared to that with EV, B_k, is expressed as

$$\begin{aligned} B_k &= \left(\frac{T_{MU} - T_{SU}}{T_{SU}}\right) C_{SU,k} - T_{MU}\left(M \log_2 U - \log_2 \Lambda_{\Phi_l,k}\right) \\ &= (U-1) C_{SU,k} - \frac{U}{K}\left(M \log_2 U - \log_2 \Lambda_{\Phi_l,k}\right), \end{aligned} \tag{20}$$

where the derivation is obtained using the relationship that $T_{MU} = U/K$ and $T_{SU} = 1/K$. When B_k is greater than zero, BD outperforms EV in SU-MIMO. We can see that the superiority of ATR over SU-MIMO depends on the number of the supported MTs in the l-th time slot, U, the number of the receive antennas, M, and the decay factor product, $\Lambda_{\Phi_l,k}$.

Therefore, the AP can determine the ATR with BD by user selection and controlling the time duration and the number of the supported MTs. (18) is rewritten using U and K as

$$C_{MU,\Phi_l,k} \approx U C_{SU,k} - \frac{U}{K}\left(M \log_2 U - \log_2 \Lambda_{\Phi_l,k}\right), \tag{21}$$

The total ATR with BD for subset Φ_l and the sum-rate for combination, Ψ, are expressed as

$$C_{MU,\Phi_l} \approx U C_{SU,\Phi_l} - \frac{U^2 M}{K} \log_2 U + \frac{U}{K} \log_2 \prod_{i \in \Phi_l} \Lambda_{\Phi_l,i}. \tag{22}$$

$$C_{MU,\Psi} \approx U C_{SU} - \frac{U^2 ML}{K} \log_2 U + \frac{U}{K} \log_2 \prod_{l=1}^{L} \prod_{i \in \Phi_l} \Lambda_{\Phi_l,i}. \tag{23}$$

The accuracy of the estimated ATR depends on the assumption in (15). We show the accuracy of ATR estimation in Sect. 5.1. Therefore, when the AP knows the ATR in SU-MIMO, $C_{SU,k}$, the ATR with BD is determined by the decay factor product, $\Lambda_{\Phi_l,k}$.

3.2 Decay Factor Product

In this subsection, we focus on the decay factor product. The decay factor product is calculated using the determinant of the correlation matrix of the null space channel matrix, $\mathbf{H}_k \tilde{\mathbf{V}}_{\Phi,k}^{(n)}$, as

$$\left|\mathbf{H}_k \tilde{\mathbf{V}}_{\Phi,k}^{(n)} \tilde{\mathbf{V}}_{\Phi,k}^{(n)H} \mathbf{H}_k^H\right| = \prod_{i=1}^{M} \bar{\lambda}_{\Phi,k,i} = \Lambda_{\Phi,k} \prod_{i=1}^{M} \lambda_{k,i}. \tag{24}$$

Here, the left side in (24) is rewritten as

$$\begin{aligned} &\left|\mathbf{H}_k \tilde{\mathbf{V}}_{\Phi,k}^{(n)} \tilde{\mathbf{V}}_{\Phi,k}^{(n)H} \mathbf{H}_k^H\right| \\ &= |\mathbf{U}_k|\,|\mathbf{\Sigma}_k| \left|\mathbf{V}_k^{(s)H} \tilde{\mathbf{V}}_{\Phi,k}^{(n)} \tilde{\mathbf{V}}_{\Phi,k}^{(n)H} \mathbf{V}_k^{(s)}\right| |\mathbf{\Sigma}_k| \left|\mathbf{U}_k^H\right| \\ &= \left|\mathbf{V}_k^{(s)H} \tilde{\mathbf{V}}_{\Phi,k}^{(n)} \tilde{\mathbf{V}}_{\Phi,k}^{(n)H} \mathbf{V}_k^{(s)}\right| \prod_{i=1}^{M} \lambda_{k,i}. \end{aligned} \tag{25}$$

Therefore, the following relationship is derived from (24) and (25).

$$\Lambda_{\Phi,k} = \left|\mathbf{V}_k^{(s)H} \tilde{\mathbf{V}}_{\Phi,k}^{(n)} \tilde{\mathbf{V}}_{\Phi,k}^{(n)H} \mathbf{V}_k^{(s)}\right|. \tag{26}$$

The decay factor product expresses the correlation of the transmission subspace and the null subspace. Since the decay factor product is the determinant of the correlation matrix of $\mathbf{V}_k^{(s)H} \tilde{\mathbf{V}}_{\Phi,k}^{(n)}$, $\Lambda_{\Phi,k}$ is a nonnegative value. When the transmission subspace, $\mathbf{V}_k^{(s)}$, is orthogonal to the null subspace, $\tilde{\mathbf{V}}_{\Phi,k}^{(n)}$, the decay factor product becomes one. In this case, (23) shows that the sum rate in BD is maximized. It is clear from (23) that the sum rate in BD becomes minus infinity when the decay factor product becomes zero. This is because the approximations of (16) and (17) are not satisfied due to inequality $\bar{\lambda}_{\Phi,k,i} \ll 1$.

Using this decay factor product, the ATR with BD is obtained by (21). We consider an additional technique to reduce the computational load. Here, matrix $\mathbf{\Gamma}_{\Phi,k} \in \mathbb{C}^{N \times N}$ is defined using $\mathbf{V}_k^{(s)}$ and $\tilde{\mathbf{V}}_{\Phi,k}^{(n)}$ as

$$\mathbf{\Gamma}_{\Phi,k} = \begin{pmatrix} \mathbf{V}_k^{(s)} & \mathbf{V}_k^{(n)} \end{pmatrix}^H \begin{pmatrix} \tilde{\mathbf{V}}_{\Phi,k}^{(s)} & \tilde{\mathbf{V}}_{\Phi,k}^{(n)} \end{pmatrix}$$

$$= \begin{pmatrix} \mathbf{V}_k^{(s)H}\tilde{\mathbf{V}}_{\Phi,k}^{(s)} & \mathbf{V}_k^{(s)H}\tilde{\mathbf{V}}_{\Phi,k}^{(n)} \\ \mathbf{V}_k^{(n)H}\tilde{\mathbf{V}}_{\Phi,k}^{(s)} & \mathbf{V}_k^{(n)H}\tilde{\mathbf{V}}_{\Phi,k}^{(n)} \end{pmatrix}. \quad (27)$$

Since $\begin{pmatrix} \mathbf{V}_k^{(s)} & \mathbf{V}_k^{(n)} \end{pmatrix}$ and $\begin{pmatrix} \tilde{\mathbf{V}}_{\Phi,k}^{(s)} & \tilde{\mathbf{V}}_{\Phi,k}^{(n)} \end{pmatrix}$ are unitary matrices, $\mathbf{\Gamma}_{\Phi,k}$ is a unitary matrix. Thus, the following equation is satisfied.

$$\begin{aligned}
&\mathbf{\Gamma}_{\Phi,k}\mathbf{\Gamma}_{\Phi,k}^H \\
&= \begin{pmatrix} \mathbf{V}_k^{(s)H}\tilde{\mathbf{V}}_{\Phi,k}^{(s)} & \mathbf{V}_k^{(s)H}\tilde{\mathbf{V}}_{\Phi,k}^{(n)} \\ \mathbf{V}_k^{(n)H}\tilde{\mathbf{V}}_{\Phi,k}^{(s)} & \mathbf{V}_k^{(n)H}\tilde{\mathbf{V}}_{\Phi,k}^{(n)} \end{pmatrix} \begin{pmatrix} \mathbf{V}_k^{(s)H}\tilde{\mathbf{V}}_{\Phi,k}^{(s)} & \mathbf{V}_k^{(s)H}\tilde{\mathbf{V}}_{\Phi,k}^{(n)} \\ \mathbf{V}_k^{(n)H}\tilde{\mathbf{V}}_{\Phi,k}^{(s)} & \mathbf{V}_k^{(n)H}\tilde{\mathbf{V}}_{\Phi,k}^{(n)} \end{pmatrix}^H \\
&= \begin{pmatrix} \mathbf{V}_k^{(s)H}\tilde{\mathbf{V}}_{\Phi,k}^{(s)}\tilde{\mathbf{V}}_{\Phi,k}^{(s)H}\mathbf{V}_k^{(s)} + \mathbf{V}_k^{(s)H}\tilde{\mathbf{V}}_{\Phi,k}^{(n)}\tilde{\mathbf{V}}_{\Phi,k}^{(n)H}\mathbf{V}_k^{(s)} \\ \mathbf{V}_k^{(n)H}\tilde{\mathbf{V}}_{\Phi,k}^{(s)}\tilde{\mathbf{V}}_{\Phi,k}^{(s)H}\mathbf{V}_k^{(s)} + \mathbf{V}_k^{(n)H}\tilde{\mathbf{V}}_{\Phi,k}^{(n)}\tilde{\mathbf{V}}_{\Phi,k}^{(n)H}\mathbf{V}_k^{(s)} \end{pmatrix} \\
&\qquad \begin{pmatrix} \mathbf{V}_k^{(s)H}\tilde{\mathbf{V}}_{\Phi,k}^{(s)}\tilde{\mathbf{V}}_{\Phi,k}^{(s)}\mathbf{V}_k^{(n)H} + \mathbf{V}_k^{(s)H}\tilde{\mathbf{V}}_{\Phi,k}^{(n)}\tilde{\mathbf{V}}_{\Phi,k}^{(n)H}\mathbf{V}_k^{(n)} \\ \mathbf{V}_k^{(n)H}\tilde{\mathbf{V}}_{\Phi,k}^{(s)}\tilde{\mathbf{V}}_{\Phi,k}^{(s)H}\mathbf{V}_k^{(n)} + \mathbf{V}_k^{(n)H}\tilde{\mathbf{V}}_{\Phi,k}^{(n)}\tilde{\mathbf{V}}_{\Phi,k}^{(n)H}\mathbf{V}_k^{(n)} \end{pmatrix} \\
&= \begin{pmatrix} \mathbf{I}_M & \mathbf{0} \\ \mathbf{0} & \mathbf{I}_{N-M} \end{pmatrix}. \quad (28)
\end{aligned}$$

By using the equalities in the second and third lines of (28), the relationship between the signal space and null space vectors is found as

$$\mathbf{V}_k^{(s)H}\tilde{\mathbf{V}}_{\Phi,k}^{(n)}\tilde{\mathbf{V}}_{\Phi,k}^{(n)H}\mathbf{V}_k^{(s)} = \mathbf{I}_M - \mathbf{V}_k^{(s)H}\tilde{\mathbf{V}}_{\Phi,k}^{(s)}\tilde{\mathbf{V}}_{\Phi,k}^{(s)H}\mathbf{V}_k^{(s)} \quad (29)$$

and (24) is rewritten as

$$\Lambda_{\Phi,k} = \left|\mathbf{I}_M - \mathbf{V}_k^{(s)H}\tilde{\mathbf{V}}_{\Phi,k}^{(s)}\tilde{\mathbf{V}}_{\Phi,k}^{(s)H}\mathbf{V}_k^{(s)}\right|. \quad (30)$$

Therefore, the decay factor product, $\Lambda_{\Phi,k}$, is calculated using the signal space of MT k, $\mathbf{V}_k^{(s)}$, and the signal space of the aggregate channel matrix corresponding to subset Φ except for MT k, $\tilde{\mathbf{V}}_{\Phi,k}^{(s)}$. Although ATR estimation based on (6) requires the calculation of $\tilde{\mathbf{V}}_{\Phi,k}^{(n)}$, (21) and (30) clarify that the calculation can be dropped. Gram-Schmidt orthogonalization calculates $\tilde{\mathbf{V}}_{\Phi,k}^{(s)}$ with less computational load compared to calculating both $\tilde{\mathbf{V}}_{\Phi,k}^{(s)}$ and $\tilde{\mathbf{V}}_{\Phi,k}^{(n)}$. Furthermore, when the number of supported MTs is two and $\Phi = \{k, j\}$, the following relationship is satisfied.

$$\begin{aligned}
\Lambda_{\Phi,k} &= \left|\mathbf{I}_M - \mathbf{V}_k^{(s)H}\tilde{\mathbf{V}}_{\Phi,k}^{(s)}\tilde{\mathbf{V}}_{\Phi,k}^{(s)H}\mathbf{V}_k^{(s)}\right| \\
&= \left|\mathbf{I}_M - \mathbf{V}_k^{(s)H}\mathbf{V}_j^{(s)}\mathbf{V}_j^{(s)H}\mathbf{V}_k^{(s)}\right| \\
&= \left|\mathbf{I}_M - \mathbf{V}_j^{(s)H}\mathbf{V}_k^{(s)}\mathbf{V}_k^{(s)H}\mathbf{V}_j^{(s)}\right| \\
&= \Lambda_{\Phi,j}. \quad (31)
\end{aligned}$$

In this case, the computational load is significantly reduced since the decay factor products for both MTs become identical.

4. User Selection Method

In this section, we evaluate the performance of user selection methods based on the proposed eigenvalue decay factor and the conventional measure. The previous section showed that the eigenvalue decay factor is the key to ATR with BD. Before transmission, the AP must choose one of N_c combinations, $\Psi_1, \ldots, \Psi_{Nc}$, where N_c is the number of possible MT combinations. When the number of MTs is K, N_c is expressed as

$$N_c = \frac{\begin{pmatrix} K \\ U \end{pmatrix}\begin{pmatrix} K-U \\ U \end{pmatrix}\cdots\begin{pmatrix} U \\ U \end{pmatrix}}{L!}. \quad (32)$$

For example, when $K = 20$ and $U = 4$, N_c becomes about 1.3×10^{10}. It is not realistic to estimate the ATR for all possible combinations. This leads to the proposal of user selection methods that select an additional MT iteratively [18]. The iterative user selection methods search through only $(K^2 - K)/2$ MT combinations or so, far fewer than the exhaustive search method. Our approach is to apply the decay factor products to an iterative user selection method.

Table 1 US-D algorithm.

1) Set $l = 1$ and $\Omega = \{1, 2, \cdots, K\}$. Calculate the right singular vectors for each MT, $\mathbf{V}_k^{(s)}$, where $k \in \Omega$.
2) If $\Omega \neq \{\}$
   Set $i = 1$ and select MT ζ as the first MT at l-th time slot from Ω arbitrarily. Set $\Phi_l = \{\zeta\}$, $\Omega = \Omega \setminus \{\zeta\}$.
   Else end.
3) If $i < U$
a) $i = i + 1$
b) For every $k \in \Omega$
· Set $\Phi_l^k = \Phi_l \cup \{k\}$
· Calculate $\tilde{\mathbf{V}}_{\Phi_l^k,j}^{(s)}$ where $j \in \Phi_l^k$ using Gram-Schmidt orthogonalization, and the decay factor product for subset Φ_l^k as $\Lambda_{all,k} = \prod_{j=1}^{i}\left|\mathbf{I}_M - \mathbf{V}_j^{(s)H}\tilde{\mathbf{V}}_{\Phi_l^k,j}^{(s)}\tilde{\mathbf{V}}_{\Phi_l^k,j}^{(s)H}\overline{\mathbf{V}}_j^{(s)}\right|$.
c) Select MT ξ that $\xi = \arg\max_{k\in\Omega}\Lambda_{all,k}$ as the i-th MT in the l-th time slot. Set $\Phi_l = \Phi_l \cup \{\xi\}$, $\Omega = \Omega \setminus \{\xi\}$, and go to Step 3.
Else set $l = l + 1$ and go to Step 2.

4.1 User Selection Based on Decay Factor Product (US-D)

The proposed User Selection method based on Decay factor product (US-D) finds the suboptimal user set while greatly reducing the number of candidate MT combinations. Table 1 lists its algorithm. Consider the selection of the i-th MT for the l-th time slot. Let Ω and Φ_l denote the subset of MTs that are not selected and that of selected $(i-1)$ MTs for the l-th time slot, respectively. When $i = 1$, the first MT is selected arbitrarily from Ω. Φ_l is defined as $\{\phi_l(1), \ldots, \phi_l(i-1)\}$. When MT k is a candidate for the i-th MT in subset Φ_l, temporal subset Φ_l^k is determined as $\Phi_l \cup \{k\}$, where Φ_l^k consists of i MTs and $k = \phi_l^k(i)$. Here, $k \in \Omega$. The signal space of all selected MTs except for the MT j in subset Φ_l^k where $j \in \Phi_l^k$, $\tilde{\mathbf{V}}_{\Phi_l^k,j}^{(s)}$ is obtained as the column basis of the aggregate signal spaces

Table 2 SUS-D algorithm.

1) Set $l = 1$ and $\Omega = \{1, 2, \cdots, K\}$. Calculate the right singular vectors for each MT, $\mathbf{V}_k^{(s)}$, where $k \in \Omega$.
2) If $\Omega \neq \{\}$
   Set $i = 1$ and select MT ζ as the first MT in the l-th time slot from Ω arbitrarily. Set $\Phi_l = \{\zeta\}$, $\Omega = \Omega \setminus \{\zeta\}$ and $\mathbf{V} = \mathbf{V}_\zeta^{(s)}$.
   Else end.
3) If $i < U$
a) $i = i + 1$
b) For every $k \in \Omega$
c) Calculate base vectors $\mathbf{V}$ using $\mathbf{V}_k^{(s)}$ where $k \in \Phi$ and the decay factor product for MT k as $\Lambda_k = \left|\mathbf{I}_M - \mathbf{V}_k^{(s)H}\mathbf{V}\mathbf{V}^H\mathbf{V}_k^{(s)}\right|$
d) Select the MT that $\xi = \arg\max_{k\in\Omega} \Lambda_k$. Set $\Phi_l = \Phi_l \cup \{\xi\}$, $\Omega = \Omega \setminus \{\xi\}$. Calculate $\mathbf{V}$ as the base vectors of the aggregate signal spaces vectors, $\left(\mathbf{V} \quad \mathbf{V}_\xi^{(s)H}\right)$, using Gram-Schmidt orthogonalization and go to Step 3.
Else, set $l = l + 1$ and go to Step 2.

vectors. When $\Phi_l^k = \{1\ 2\ \cdots\ i\}$, $\tilde{\mathbf{V}}_{\Phi_l^k,j}^{(s)}$ is calculated as the base vectors by subjecting the aggregate signal space vectors, $\tilde{\mathbf{V}}_{\Phi_l^k,j}^{(s)} = \left(\mathbf{V}_{\Phi_l^k,1}^{(s)} \cdots \mathbf{V}_{\Phi_l^k,j-1}^{(s)} \mathbf{V}_{\Phi_l^k,j+1}^{(s)} \cdots \mathbf{V}_{\Phi_l^k,i}^{(s)}\right)$, to Gram-Schmidt orthogonalization. The product of the decay factor products, $\Lambda_{all,k}$, is then calculated for additional MT k as

$$\Lambda_{all,k} = \prod_{j\in\Phi_l^k} \Lambda_{\Phi_l^k,j}, \tag{33}$$

where $\Lambda_{\Phi_l^k,j} = \left|\mathbf{I}_M - \mathbf{V}_j^{(s)}\tilde{\mathbf{V}}_{\Phi_l^k,j}^{(s)}\tilde{\mathbf{V}}_{\Phi_l^k,j}^{(s)}\mathbf{V}_j^{(s)}\right|$. The AP selects the i-th MT that maximizes $\Lambda_{all,k}$ for the l-th time slot.

4.2 Simple User Selection Based on Decay Factor (SUS-D)

The Simplified proposed User Selection method based on Decay factor product (SUS-D) is shown in Table 2. SUS-D ignores the ATR degradation for the already selected users to reduce the calculation complexity while US-D calculates the ATR degradation corresponding to all the selected MTs so as to select more appropriate MT subsets. SUS-D enables the AP to determine the combination with much lower computational load. In SUS-D, the signal space of the selected MTs $\mathbf{V}$ is calculated as the base vectors of the aggregate signal space vectors which consist of the signal vectors of the selected MTs. When $\Phi_l = \{1, 2, \ldots, i-1\}$, $\mathbf{V}$ is obtained using Gram-Schmidt orthogonalization for $\mathbf{V} = \left(\mathbf{V}_1^{(s)}\ \mathbf{V}_2^{(s)}\ \cdots\ \mathbf{V}_{i-1}^{(s)}\right)$. In other words, $\mathbf{V}$ is equal to $\tilde{\mathbf{V}}_{\Phi_l^k,i}^{(s)}$ in Step 3(b) for US-D. SUS-D does not require the calculation of $\tilde{\mathbf{V}}_{\Phi_l^k,j}^{(s)}$ for $j < i$. The decay factor product, Λ_k, is calculated using (30) for the additional MT, MT k, as

$$\Lambda_k = \left|\mathbf{I}_M - \mathbf{V}_k^{(s)H}\mathbf{V}\mathbf{V}^H\mathbf{V}_k^{(s)}\right|, \tag{34}$$

The AP selects the i-th MT in the l-th time slot that maximizes the decay factor product, Λ_k. Since the AP calculates just the decay factor product for one additional MT, the computational load is greatly reduced. SUS-D makes the decay factor product for all MTs in the subset, $\Lambda_{all,k}$, a function of the decay factor product for the additional MT, Λ_k and $\arg_k \max_{k\in\Omega} \Lambda_k \approx \arg_k \max_{k\in\Omega} \Lambda_{all,k}$.

Note that the algorithms of US-D and SUS-D are identical when the number of MTs in the same time slot is 2 since $\Lambda_{all,k} = \Lambda_1^2 = \Lambda_2^2$.

Table 3 US-C algorithm.

1) Set the serial of the time slot, $l = 1$, the serial of the selected MT in the l-th time slot, and $\Omega = \{1, 2, \cdots, K\}$. Calculate the right singular vectors for each MT, $\mathbf{V}_k^{(s)}$, where $k \in \Omega$, and the ATR with EV, $C_{s,k} = \log_2\left|\mathbf{I}_M + \mathbf{H}_k\mathbf{V}_k^{(s)}\mathbf{P}_{s,k}^2\mathbf{V}_k^{(s)H}\mathbf{H}_k^H\right|$
2) If $\Omega \neq \{\}$
   Set $i = 1$ and select the MT that $\zeta = \arg\max_{k\in\Omega} \log_2 C_{s,k}$. Set $\Phi_l = \{\zeta\}$, $\Omega = \Omega \setminus \{\zeta\}$.
   Else end.
3) If $i < U$
a) $i = i + 1$
b) For every $k \in \Omega$
- Set $\Phi_l^k = \Phi_l \cup \{k\}$
- Calculate the right singular vectors for null space, $\tilde{\mathbf{V}}_{\Phi_l^k,j}^{(n)}$ and perform SVD on $\mathbf{H}_j\tilde{\mathbf{V}}_{\Phi_l^k,j}^{(n)}$ for every $j \in \Phi_l^k$.
- Apply water-filling strategy over $\bar{\lambda}_{\Phi_l^k,j,1}, \cdots, \bar{\lambda}_{\Phi_l^k,j,M}$ and find the power allocation matrix $\mathbf{P}_j$.
- Calculate the ATRs for the subset Φ_l^k as $C_{l,k} = \sum_{j\in\Phi_l^k} \log_2\left|\mathbf{I}_M + \mathbf{H}_j\tilde{\mathbf{V}}_{\Phi_l^k,j}^{(n)}\mathbf{P}_{\Phi_l^k,j}^2\tilde{\mathbf{V}}_{\Phi_l^k,j}^{(n)H}\mathbf{H}_j^H\right|$

c) Select the MT that $\xi = \arg\max_{k\in\Omega} C_{l,k}$. Set $\Phi_l = \Phi_l \cup \{\xi\}$, $\Omega = \Omega \setminus \{\xi\}$, and go to Step 3.
Else, set $l = l + 1$ and go to Step 2.

4.3 User Selection Based on Channel Capacity (US-C)

Table 3 lists the algorithm of the conventional User Selection method based on channel Capacity (US-C). US-C selects an additional MT from the remaining unselected MTs so as to maximize the ATR. Since US-C requires SVD at Step 3-(b) to calculate the eigenvalues, the computational load is excessive. When all MTs can be expected to have the same SNR, US-C selects suboptimal combinations of the MTs.

4.4 User Selection Based on Channel Norm (US-N)

User Selection method based on channel Norm (US-N) also selects an additional MT from the remaining unselected MTs, but US-N uses the channel Frobenius norm in null space for the other MTs of the subset at Step (3)-b. The AP selects the additional MT that maximizes the summation of the Frobenius norm of the channel in null space, $\sum_{j\in\Phi_l^k} \left\|\mathbf{H}_j\mathbf{V}_{\Phi_l^k,j}^{(n)}\mathbf{V}_{\Phi_l^k,j}^{(n)H}\mathbf{H}_j\right\|_F^2$. The computational load of US-N

Table 4 US-N algorithm.

1) Set the serial of the time slot, $l = 1$, the serial of the selected MT in the l-th time slot, and $\Omega = \{1, 2, \cdots, K\}$. Calculate the right singular vectors for each MT, $\mathbf{V}_k^{(s)}$, where $k \in \Omega$.
2) If $\Omega \neq \{\}$
   Set $i = 1$ and select the MT that $\zeta = \arg\max_{k\in\Omega} \log_2 C_{s,k}$.
   Set $\Phi_l = \{\zeta\}$, $\Omega = \Omega \setminus \{\zeta\}$, and $\mathbf{V} = \mathbf{V}_\zeta^{(s)}$.
   Else end.
3) If $i < U$
a) $i = i + 1$
b) For every $k \in \Omega$
· Calculate $\overline{\mathbf{H}}_k = \mathbf{H}_k - \mathbf{H}_k\mathbf{V}\mathbf{V}^H$ and set $\Phi_l^k = \Phi_l \cup \{\xi\}$.
· For j =1: i–1
· Calculate $\widetilde{\mathbf{V}}_{\Phi_l^k,j}^{(s)}$ where $j \in \Phi_l$ as the base vectors for the aggregate signal space vectors that consist of $\left\{\mathbf{V}_{\phi_l^k(1)}^{(s)} \cdots \mathbf{V}_{\phi_l^k(\iota-1)}^{(s)} \; \mathbf{V}_{\phi_l^k(\iota+1)}^{(s)} \cdots \mathbf{V}_{\phi_l^k(i)}^{(s)}\right\}$, where $j = \phi_l^k(\iota)$, using Gram-Schmidt orthogonalization.
· Calculate $\overline{\mathbf{H}}_j = \mathbf{H}_j - \mathbf{H}_j\widetilde{\mathbf{V}}_{\Phi_l^k,j}^{(s)}\widetilde{\mathbf{V}}_{\Phi_l^k,j}^{(s)H}$.
· Select the MT that $\xi = \arg\max_{k\in\Omega}\left(\left\|\overline{\mathbf{H}}_k\right\|_F^2 + \sum_{j\in\Phi_l}\left\|\overline{\mathbf{H}}_j\right\|_F^2\right)$. Set $\Phi_l = \Phi_l \cup \{\xi\}$ and $\Omega = \Omega \setminus \{\xi\}$.
· Select $\mathbf{V}$ as $\widetilde{\mathbf{V}}_{\Phi_l^k,j}^{(s)}$ and go to Step 3.
Else, set $l = l + 1$ and go to Step 2.

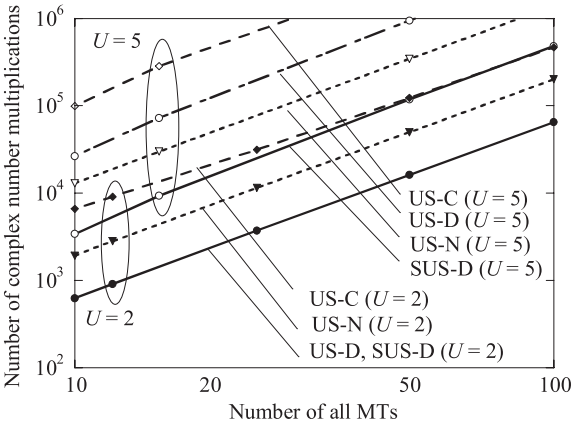

Fig. 1 Comparison of computational loads when (N, M, U) = (4, 2, 2) and (N, M, U) = (10, 2, 5).

is much less than that of US-C in [18]. The processing flow is listed in Table 4.

4.5 Computational Load Comparison

To estimate the computational loads of the user selection methods, we use the metric of the number of complex number multiplications. In this subsection, we consider the computational load of Step 3 in US-D, SUS-D, US-N, and US-C, since this step dominates the other steps. Figure 1 shows the numbers of complex number multiplications versus the number of MTs in two scenarios where the number of receive antennas, transmit antennas, and the MTs in each subset, (N, M, U), are (4, 2, 2) and (10, 2, 5). When the number of the MTs in the same time slot, U, is two, US-D and SUS-D have about 66% lower computational load than US-N and 91% lower load than US-C. When $U = 5$, the calculation load of US-D exceeds that of US-N. However, SUS-D has the lowest computational load. The calculation load of SUS-D is 74% and 97% lower that of US-N and US-C, respectively.

5. Simulation Results

The effectiveness of US-D and SUS-D was evaluated by computer simulations. We assumed that the channel matrix between the AP and the MT k, $\mathbf{H}_k$, was a spatially uncorrelated Rayleigh fading channel model and each element of $\mathbf{H}_k$ behaved as an independent and identically distributed (i.i.d.) complex Gaussian variable with zero mean. The number of transmit antennas was taken as N. The expectation of the noise power at the receive antennas and the expected average power of each element in $\mathbf{H}_k$ were set to one and Γ_k, respectively. Since the transmission power, P, was assumed to be one, Γ_k expresses the expectation of the received SNR between the AP and MT k in a Single Input Single Output (SISO) channel. We assumed that the environment was quasi-static.

5.1 Accuracy of Capacity Estimation Based on Decay Factors

First, we show the estimation accuracy of the calculated ATR by using the decay factors from (21). Figure 2(a) shows the relationship between the ATR for BD given in (6) and that estimated using the decay factor products in (21). The number of receive antennas, transmit antennas, and MTs of each subset are one, three, and three, respectively. The expected SNR is assumed to be 25 dB. As ATR falls, the estimated ATR decreases compared to the actual ATR. This is because the assumption in (15) is not satisfied.

Figure 2(b) shows the ATRs when the number of receive antennas, transmit antennas, and MTs in each subset are two, six, and three, respectively. Compared to (a), the difference between the estimated ATR and the actual one becomes large at low ATR values. Since (15) is the only assumption in the ATR estimation by (23), the degradation in estimation accuracy is caused by the decrease in eigenvalues.

We note, however, that estimation accuracy is very high when ATR is high. Since the MTs that have high ATRs are identified in user selection, the estimation error does not impact the effectiveness of US-D.

5.2 Achievable Transmission Rate for Single Receive Antenna MTs

The ATRs for US-D, US-C, and US-N were evaluated. We assumed that the number of all MTs, K, was 100 and that

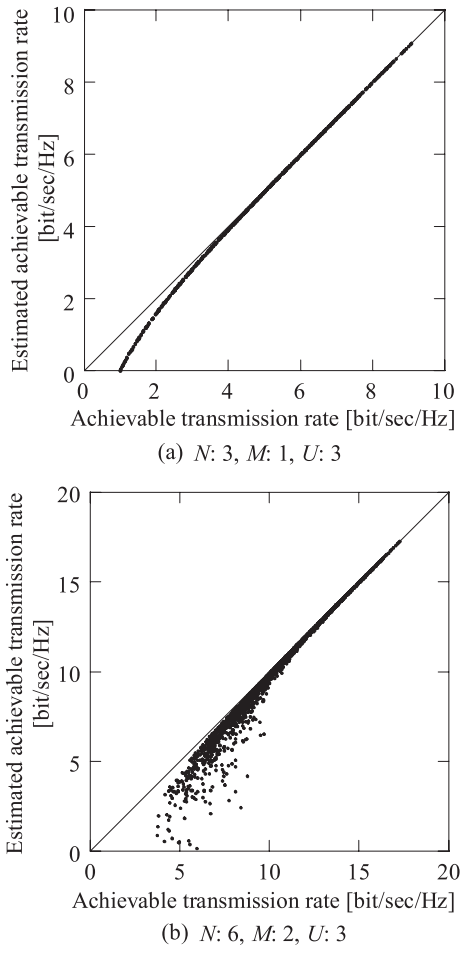

Fig. 2 Achievable transmission rate versus estimated achievable transmission rate.

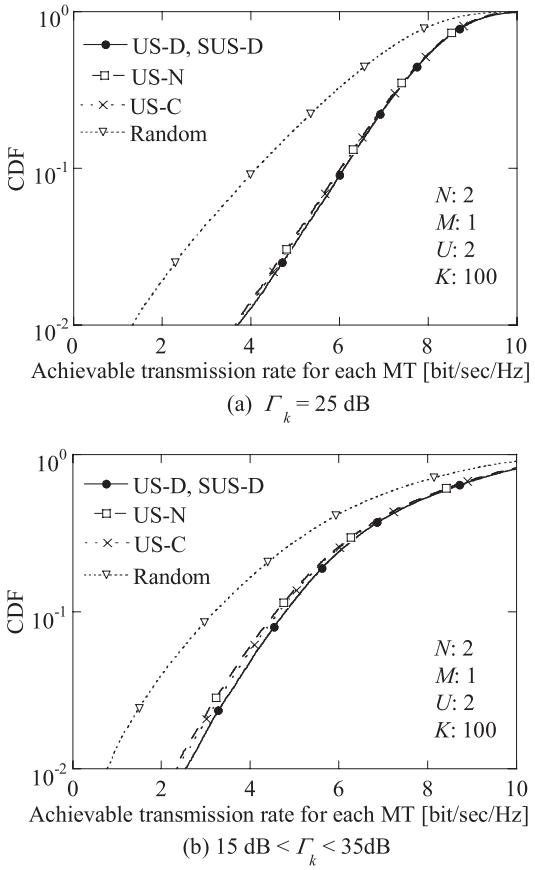

Fig. 3 CDFs of achievable transmission rate when K =100.

the expected SNR was 25 dB (Γ_k = 25 dB, $1 \le k \le K$). In each time slot, the AP communicates with two MTs, U = 2. As shown in Sect. 4.2, ATR for SUS-D is the same as that for US-D when U = 2. Figure 3 shows the Cumulative Distribution Functions (CDFs) of the ATRs of each MT for the combinations of the MTs yielded by the user selection methods.

In Fig. 3(a), the number of transmit and receive antennas are two and one, respectively. The line marked 'Random' plots the CDF of the ATRs for randomly chosen combinations. It is found that among the user selection methods examined, US-D, US-C, and US-N offer almost the same ATRs. The ATR at 10% outage for these user selection methods is 1.9 bit/sec/Hz greater than that achieved with random selection. It is found that user selection schemes based on capacity, norm, and correlation yield identical performance when all MTs have the same expected SNR. This is because all parameters express the degradation in the power of the channel when the number of receive antennas is one.

Figure 3(b) shows the ATRs in the environment in which Γ_k was randomly set from 15 dB to 35 dB (25 ± 10 dB). In this scenario, the performances differ with the user selection method. US-D has the highest ATR and US-C has the second highest ATR. The ATR at 10% outage for US-D is 1.6 bit/sec/Hz greater than that achieved with random selection. In this scenario, the ATR at 10% outage for US-D is 1.20 and 1.15 times greater than those of US-N and US-C, respectively.

The reason why US-D is superior to the conventional user selection methods is given by (21). US-C and US-N select the MT corresponding to the highest ATR. (21) shows that the ATR with BD, $C_{MU,\Phi_l,k}$, becomes large when the ATR with EV, $C_{SU,k}$, increases. Thus, the AP likely chooses the MTs that have the highest ATR in SU-MIMO and ignores the degradation in ATR due to the correlation between signal spaces of the selected MTs. Although the conventional user selection methods, US-C and US-N, improve the ATR in the earlier time slots, the ATR in the later part becomes low and the sum rate in (23), $C_{MU,\Psi}$, is degraded because of the high correlation of the signal spaces. On the other hand, US-D determines the scheduling so as to reduce the correlation of the signal spaces among the selected MTs in each time slot. Therefore, US-D improves the sum rate since the term $\log_2 \prod_{l=1}^{L} \prod_{i \in \Phi_l} \Lambda_{\Phi_l,i}$ in (23) is maximized.

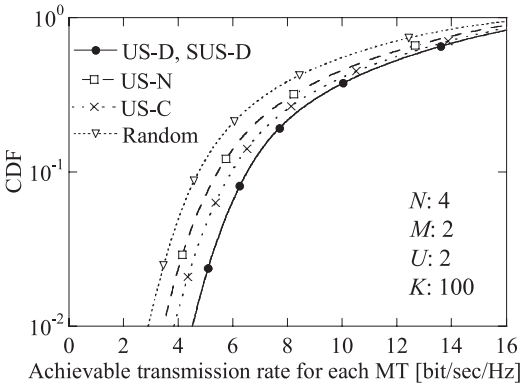

Fig. 4 CDFs of achievable transmission rate when $N = 4$, $M = 2$, $U = 2$, $K = 100$ and $15\,\text{dB} \le \Gamma_k \le 35\,\text{dB}$.

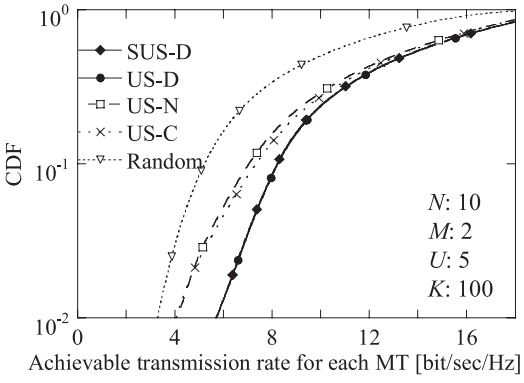

Fig. 5 CDFs of achievable transmission rate when $N = 10$, $M = 2$, $U = 5$, K =100 and $15\,\text{dB} \le \Gamma_k \le 35\,\text{dB}$.

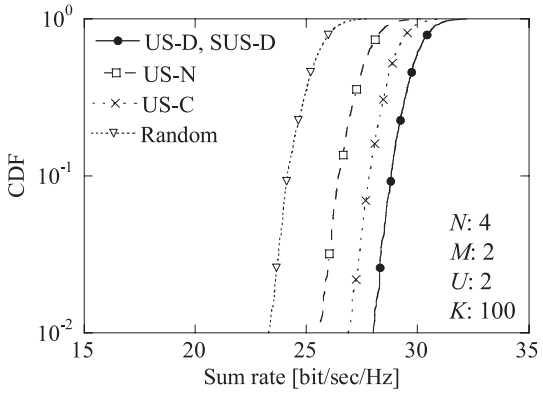

Fig. 6 CDFs of sum rates when $K = 100$, $N = 4$, $M = 2$, $U = 2$, and $15\,\text{dB} \le \Gamma_k \le 35\,\text{dB}$.

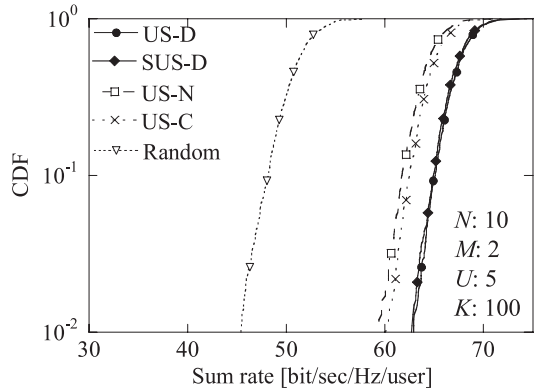

Fig. 7 CDFs of sum rates when $K = 100$, $N = 10$, $M = 2$, $U = 5$, and $15\,\text{dB} \le \Gamma_k \le 35\,\text{dB}$.

5.3 Achievable Transmission Rate for Two Receive Antenna MTs

Figure 4 shows the CDFs of the ATR when the number of transmit and receive antennas are four and two. The number of MTs was 100 and the expected SNR was set between 15 dB and 35 dB. In this scenario, US-D (SUS-D) outperforms the other user selection methods. The 10% outage ATRs of US-D, US-C, and US-N are, respectively, 1.8, 1.2, and 0.7 bit/sec/Hz greater than that of random selection. Since US-C selects the MTs corresponding to high ATR for the earliest subsets, the ATRs of the MTs placed in the last few subsets are degraded.

Figure 5 shows the CDFs of the ATR when the numbers of MTs in each subset is 5. Γ_k is set between 15 dB and 35 dB and the numbers of transmit and receive antennas are ten and two, respectively. The 10% outage ATRs for US-D, SUS-D, US-C, US-N are, respectively, 3.0, 3.0, 2.1 and 1.8 bit/sec/Hz greater than that of random selection. The difference in the ATR between US-C and US-N becomes small and the superiority of US-D and SUS-D increases. In Fig. 5, we can see that the ATR degradation for SUS-D relative to US-D is negligible while the computational load is reduced.

It is found that the improvement of US-D becomes large compared to the single receive antenna cases. Since $\Lambda_{\Phi_l,k}$ is the product of the eigenvalue decay factors, the influence of $\Lambda_{\Phi_l,k}$ increases with the number of receive antennas. Thus, the influence of the decay factor product becomes large in the cases of multiple receive antennas.

5.4 Sum Rate for Selected Combination

Sects. 5.2 and 5.3 showed the CDFs of ATRs for each MT. In this section, we focus on the sum rates corresponding to the selected combinations of MTs. Compared to the ATRs for each MT, the sum rate expresses the performance of the user selection method from the operator's point of view.

Figure 6 shows the CDFs of the sum rates when the numbers of transmit and receive antennas, all MTs, and the MTs in each subset are 4, 2, 100, and 2, respectively. Γ_k is set from 15 to 35 dB. The conditions are the same as in Fig. 4. The median sum rate for US-D is 4.5, 2.4 and 1.1 bit/sec/Hz greater than those for random selection, US-N, and US-C, respectively. Figure 7 shows the CDFs of the sum rates when $M = 2$, $N = 10$, $K = 100$, $U = 5$, and $15\,\text{dB} \le \Gamma_k \le 35\,\text{dB}$. The conditions are the same as in Fig. 5. The median sum rate for US-D is 16.5, 3.3, 2.6, and 0.2 bit/sec/Hz greater than those for random selection, US-N, US-C, and SUS-D, respectively.

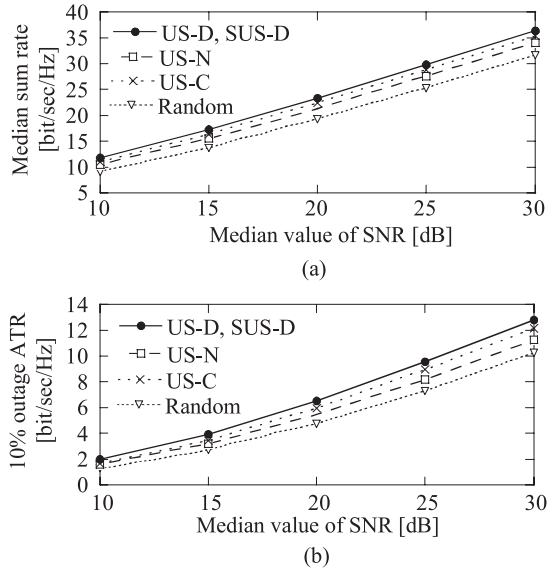

Fig. 8 Median sum rate (a) and 10% outage ATR (b) versus median SNR when $K = 100$, $N = 4$, $M = 2$, $U = 2$.

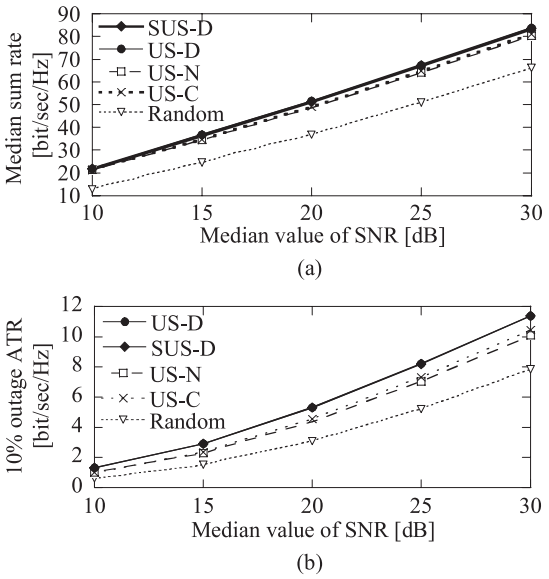

Fig. 9 Median sum rate (a) and 10% outage ATR (b) versus median SNR when $K = 100$, $N = 10$, $M = 2$, $U = 5$.

5.5 Achievable Transmission Rate and Sum Rate Versus SNR

Figure 8 shows the median sum rates and the 10% outage of ATRs versus SNR when the numbers of transmit and receive antennas, all MTs, the MTs in each subset are 4, 2, 100, and 2, respectively. Γ_k is determined from the median SNR −10 dB to the median SNR +10 dB. Thus, the ATR corresponding to the median SNR of 15 dB represents the ATR for the scenario that Γ_k lies in the range of 5 dB to 25 dB (15 ± 10 dB). This figure shows that US-D yields the highest ATR among the user selection methods examined. To obtain the median sum rate of 20 bit/sec/Hz, US-D, US-N, US-C, and random selection require the median SNRs of 17.3, 18.1, 18.8, and 21.1 dB, respectively. When the 10% outage ATR of 5 bit/sec/Hz is required, the median values of SNR for US-D, US-C, US-N, and random selection are 16.9, 18.1, 18.8, and 20.5 dB, respectively. For both 10% outage ATR and median sum rate, US-D attains the highest performance over a wide range of median SNR values.

Figure 9 shows the median sum rates and the 10% outage ATRs when the numbers of transmit and receive antennas, all MTs, and the MTs in each subset are 2, 10, 100, and 5, respectively. All the user selection methods examined offer a large improvement in sum rates over random selection. To obtain the sum rates of 50 bit/sec/Hz, US-D, US-C, US-N, and random selection require the median SNRs of 19.4, 20.2, 20.2, and 24.6 dB, respectively. When the 10% outage ATR of 5 bit/sec/Hz is required, the median SNRs for US-D, SUS-D, US-C, US-N, and random selection are 19.2, 19.2, 21.0, 21.3, and 24.5 dB, respectively.

In Sect. 5.1 of this section, it was found that the estimation accuracy achieved when using the eigenvalue decay factor deteriorates when the SNR decreases. However, Figs. 8 and 9 clarify that US-D and SUS-D have the best performance even if the SNR is low. This is because the AP can choose the MT that has sufficiently large null space eigenvalues when the number of MTs is large.

6. Conclusion

In this paper, we proposed a new user selection measure based on the relationship between the achievable transmission rate for EigenVector transmission (EV) in SU-MIMO and that for Block Diagonalization transmission (BD) in MU-MIMO when the equal power allocation strategy is applied. The new measure, the eigenvalue decay factor, represents the degradation of the eigenvalues in null space compared to those in SU-MIMO; it is obtained from the signal space vectors of the Mobile Terminals (MTs) in the physical layer. (21) gives us an intuitive understanding of the relationship between the achievable transmission rate and the eigenvalue decay factor. Since the new measure is based on MT spatial separability, the effectiveness of user selection methods with the new measure can be applied to the scenario wherein the SNR of the MTs varies; the total ATRs of the conventional methods are degraded by the SNR variations. To show the effectiveness of the new measure, the achievable transmission rates of User Selection methods with Decay factor product (US-D) and Simplified one (SUS-D) were evaluated on the assumption of the same number of supported MTs at each time slot and the same number of receive antennas. It was found that US-D and SUS-D select the combination that has the highest performance compared to user selection methods based on conventional measures and SUS-D significantly reduces the computational load.

References

[1] G.J. Foschini and M.J. Gans, "On limits of wireless communications in a fading environment when using multiple antennas," Wirel. Pers. Commun., vol.6, pp.311–335, 1998.
[2] I.E. Telatar, "Capacity of multi-antenna Gaussian channels," Eur. Trans on Telecommun. (ETT), vol.10, pp.585–595, Nov.-Dec. 1999.
[3] Q.H. Spencer, C.B. Peel, A.L. Swindlehurst, and M. Haardt, "An introduction to the multi-user MIMO downlink," IEEE Commun. Mag., vol.42, no.10, pp.60–67, Oct. 2004.
[4] M. Costa, "Writing on dirty paper," IEEE Trans. Inf. Theory, vol.29, no.3, pp.439–441, May 1983.
[5] H. Weingarten, Y. Steinberg, and S. Shamai, "The capacity region of the Gaussian MIMO broadcast channel," Proc. IEEE International Symposium on Information Theory, p.174, June-July 2004.
[6] Q.H. Spencer, A.L. Swindlehurst, and M. Haardt, "Zero-forcing methods for downlink spatial multiplexingin multiuser MIMO channels," IEEE Trans. Signal. Process., vol.52, no.2, pp.461–471, Feb. 2004.
[7] L.U. Choi and R.D. Murch, "A transmit preprocessing technique for multiuser MIMO systems using a decomposition approach," IEEE Trans. Wireless Commun., vol.3, no.1, pp.20–24, Jan. 2004.
[8] K.K. Wong, R.D. Murch, K.B. Letaief, "A joint channel diagonalization for multiuser MIMO antenna systems," IEEE Trans. Wireless Commun., vol.2, no.4, pp.773–786, July 2003.
[9] Z. Pan, K.K. Wong, and T.S. Ng, "Generalized multiuser orthogonal space-division multiplexing," IEEE Trans. Wireless Commun., vol.3, no.6, pp.1969–1973, Nov. 2004.
[10] R. Chen, J.G. Andrews, and R.W. Heath, Jr., "Multiuser space-time block coded MIMO system with downlink precoding," Proc. IEEE International Conference on Commun., vol.5, pp.2689–2693, June 2004.
[11] M. Sharif and B. Hassibi, "A comparison of time-sharing, DPC, and beamforming for MIMO broad cast channels with many users," IEEE Trans. Commun., vol.55, no.1, pp.11–15, Jan. 2007.
[12] S. Sigdel and W.A. Krzymien, "Antenna and user subset selection in downlink multiuser orthogonal space-division multiplexing," WPMC 2006 Proc., pp.671–675, Sept. 2006.
[13] T. Yoo and A. Goldsmith, "On the optimality of multiantenna broadcast scheduling using zero-forcing beamforming," IEEE J. Sel. Areas Commun., vol.24, no.3, pp.528–541, March 2006.
[14] G. Dimic and N.D. Sidiropoulos, "On downlink beamforming with greedy user selection: Performance analysis and a simple new algorithm," IEEE Trans. Signal Process., vol.53, no.10, pp.3857–3868, Oct. 2005.
[15] Z. Tu and R.S. Blum, "Multiuser diversity for a dirty paper approach," IEEE Commun. Lett., vol.7, no.8, pp.370–372, Aug. 2003.
[16] H. Yin and H. Liu, "Performance of space-division multiple-access (SDMA) with scheduling," IEEE Trans. Wireless Commun., vol.1, no.4, pp.611–618, Oct. 2002.
[17] C. Wang and R.D. Murch, "Adaptive downlink multi-user MIMO wireless systems for correlated channels with imperfect CSI," IEEE Trans. Wireless Commun., vol.5, no.9, Sept. 2006.
[18] Z. Shen, R. Chen, J.G. Andrews, R.W. Heath, Jr., and B.L. Evans, "Low complexity user selection algorithms for multiuser MIMO systems with block diagonalization," IEEE Trans. Signal Process., vol.54, no.9, Sept. 2006.
[19] S. Signel and W.A. Krzymien, "Simplified antenna selection and user scheduling for orthogonal space-divisionmultiplexing," WCNC2007 Proc., pp.1730–1735, March 2007.
[20] T. Ji, T. Yoo, and A. Goldsmith, "Low complex user selection strategies for multi-user MIMO downlink," WCNC2007 Proc., pp.1534–1539, March 2007.
[21] R. Kudo, Y. Takatori, K. Nishimori, A. Ohta, and S. Kubota, "User selection method for block diagonalization in multiuser MIMO systems," GLOBECOM'07 Proc., IEEE, Nov. 2007.
[22] L.U. Choi, M.T. Ivrlac, R.D. Murch, and W. Utschick, "On strategies of multi-user MIMO transmit signal processing," IEEE Trans. Wireless Commun., vol.3, no.6, pp.1936–1941, Nov. 2004.
[23] J.G. Proakis, Digital communications, 3rd ed., McGraw-Hill, New York, 1995.
[24] A. Paulraj, R. Nabar, and D. Gore, Introduction to Space — Time Wireless Communications, Cambridge Univ. Press, Cambridge, U.K., 2003.

Appendix

In this appendix, the j-th eigenvalue of MU-MIMO with Block Diagonalization algorithm (BD) is smaller than that of SU-MIMO. Channel matrix for a single user can be expressed as follows,

$$\mathbf{H} = \mathbf{U}\mathbf{D}\mathbf{V}^H, \tag{A·1}$$

where $\mathbf{H}$, $\mathbf{U}$, $\mathbf{D}$, and $\mathbf{V}$ are matrices of dimensions $M\times N$, $M\times M$, $M\times M$, and $N\times M$, respectively. $\mathbf{U}$ and $\mathbf{V}$ are the left and right singular vectors, and $\mathbf{D}$ is the diagonal matrix whose diagonal elements are the square roots of the eigenvalues, $\lambda_1, \lambda_2, \cdots, \lambda_M$. Here, we assume that the number of transmit antennas is greater than that of receive antennas; $N > M$.

To compare the eigenvalues of SU-MIMO to those of MU-MIMO with BD algorithm, we compare the original eigenvalues of $\mathbf{H}^H\mathbf{H}$ with those of $\mathbf{Q}^{(L)H}\mathbf{H}^H\mathbf{H}\mathbf{Q}^{(L)}$, where $\mathbf{Q}^{(L)} \in \mathbb{C}^{N\times L}$ is the left part of a unitary matrix, i.e. $\mathbf{Q} = (\mathbf{Q}^{(L)}\mathbf{Q}^{(R)})$ and $L \geq M$. $\mathbf{H}\mathbf{Q}^{(L)}$ is expressed as

$$\mathbf{H}\mathbf{Q}^{(L)} = \overline{\mathbf{U}}\,\overline{\mathbf{D}}\,\overline{\mathbf{V}}^H, \tag{A·2}$$

where $\bar{\mathbf{U}} \in \mathbb{C}^{M\times M}$ and $\bar{\mathbf{V}} \in \mathbb{C}^{L\times M}$ are the left and right singular vectors, and $\bar{\mathbf{D}} \in \mathbb{C}^{M\times M}$ is the diagonal matrix whose diagonal elements are defined as the square roots of $\bar{\lambda}_1, \bar{\lambda}_2, \cdots, \bar{\lambda}_M$. Since the eigenvalues of $\mathbf{H}^H\mathbf{H}$ are identical to those of $\mathbf{Q}^H\mathbf{H}^H\mathbf{H}\mathbf{Q}$, it should be proven that k-th eigenvalue of $\mathbf{Q}^{(L)H}\mathbf{H}^H\mathbf{H}\mathbf{Q}^{(L)}$ is smaller than that of $\mathbf{Q}^H\mathbf{H}^H\mathbf{H}\mathbf{Q}$ for arbitrary k. Here, the eigenvalues of $\mathbf{Q}^{(L)H}\mathbf{H}^H\mathbf{H}\mathbf{Q}^{(L)}$ are $\bar{\lambda}_1, \bar{\lambda}_2, \cdots \bar{\lambda}_M$. $\mathbf{Q}^H\mathbf{H}^H\mathbf{H}\mathbf{Q}$ can be rewritten as follows.

$$\begin{aligned}\mathbf{Q}^H\mathbf{H}^H\mathbf{H}\mathbf{Q} &= \left(\mathbf{Q}^{(L)} \quad \mathbf{Q}^{(R)}\right)^H \mathbf{H}^H\mathbf{H}\left(\mathbf{Q}^{(L)} \quad \mathbf{Q}^{(R)}\right) \\ &= \begin{pmatrix} \mathbf{Q}^{(L)H}\mathbf{H}^H\mathbf{H}\mathbf{Q}^{(L)H} & \mathbf{Q}^{(L)H}\mathbf{H}^H\mathbf{H}\mathbf{Q}^{(R)H} \\ \mathbf{Q}^{(R)H}\mathbf{H}^H\mathbf{H}\mathbf{Q}^{(L)H} & \mathbf{Q}^{(R)H}\mathbf{H}^H\mathbf{H}\mathbf{Q}^{(R)H} \end{pmatrix}\end{aligned} \tag{A·3}$$

To simplify the following analysis, we rewrote the above equation as follows.

$$\begin{aligned}\mathbf{G} &= \mathbf{Q}^H\mathbf{H}^H\mathbf{H}\mathbf{Q} \\ &= \begin{pmatrix} \mathbf{G}_{11} & \mathbf{G}_{12} \\ \mathbf{G}_{21} & \mathbf{G}_{22} \end{pmatrix}\end{aligned} \tag{A·4}$$

where

$$\begin{aligned}&\mathbf{G}_{11} = \mathbf{Q}^{(L)H}\mathbf{H}^H\mathbf{H}\mathbf{Q}^{(L)H},\ \mathbf{G}_{12} = \mathbf{Q}^{(L)H}\mathbf{H}^H\mathbf{H}\mathbf{Q}^{(R)H}, \\ &\mathbf{G}_{21} = \mathbf{Q}^{(R)H}\mathbf{H}^H\mathbf{H}\mathbf{Q}^{(L)H},\ \mathbf{G}_{22} = \mathbf{Q}^{(R)H}\mathbf{H}^H\mathbf{H}\mathbf{Q}^{(R)H}\end{aligned} \tag{A·5}$$

Without loss of generality, order the eigenvalues of $\mathbf{G}$ and $\mathbf{G}_{11}$ such that $\lambda_1 \geq \lambda_2 \geq \cdots \geq \lambda_M$ and $\bar{\lambda}_1 \geq \bar{\lambda}_2 \geq \cdots \geq \bar{\lambda}_M$, respectively. By using the Courant Fischer mini-max theorem, the $(j+1)$-th eigenvalue, λ_{j+1}, can be expressed as follows.

$$\lambda_{j+1} = \max_{\mathbf{V}_j^H \mathbf{x} = \mathbf{0}} \frac{\mathbf{x}^H \mathbf{G} \mathbf{x}}{\mathbf{x}^H \mathbf{x}} \tag{A·6}$$

where $\mathbf{V}_j = (\mathbf{v}_1 \mathbf{v}_2 \ldots \mathbf{v}_j)$ and $\mathbf{v}_k$ is the eigenvector for the k-th eigenvalue. To reduce the matrix size, matrix $\mathbf{E}$ is defined as follows.

$$\mathbf{E} = (\mathbf{e}_{N-L+1}\ \mathbf{e}_{N-L+2}\ \cdots\ \mathbf{e}_N) = \begin{pmatrix} \mathbf{0}_{N-L,L} \\ \mathbf{I}_L \end{pmatrix}, \tag{A·7}$$

where $\mathbf{e}_k$ is an N × 1 column vector whose k-th element is one and other elements are zero, and $\mathbf{0}_{N-L,L} \in \mathbb{C}^{(N-L)\times L}$ is a zero matrix. We also define matrices, $\mathbf{V}_j^{(u)} \in \mathbb{C}^{(N-L)\times j}$ and $\mathbf{V}_j^{(d)} \in \mathbb{C}^{L\times j}$, as

$$\mathbf{V}_j = \begin{pmatrix} \mathbf{V}_j^{(u)} \\ \mathbf{V}_j^{(d)} \end{pmatrix}. \tag{A·8}$$

Using $\mathbf{E}$ and $\mathbf{V}_j^{(u)}$, the following inequality can be derived.

$$\begin{aligned} \lambda_{j+1} &= \max_{\mathbf{V}_j^H \mathbf{x} = \mathbf{0}} \frac{\mathbf{x}^H \mathbf{G} \mathbf{x}}{\mathbf{x}^H \mathbf{x}} \geq \max_{\substack{\mathbf{V}_j^H \mathbf{x} = \mathbf{0} \\ \mathbf{E}^H \mathbf{x} = \mathbf{0}}} \frac{\mathbf{x}^H \mathbf{G} \mathbf{x}}{\mathbf{x}^H \mathbf{x}} \\ &= \max_{\mathbf{V}_j^{(u)H} \mathbf{y} = \mathbf{0}} \frac{\mathbf{y}^H \mathbf{G}_{11} \mathbf{y}}{\mathbf{y}^H \mathbf{y}}, \end{aligned} \tag{A·9}$$

where $\mathbf{y}$ is $(N-L) \times 1$ arbitrary column vector and $\bar{\mathbf{v}}_k$ is the eigenvector for eigenvalue $\bar{\lambda}_k$. The above inequality is obvious since the condition, $\mathbf{E}^H \mathbf{x} = \mathbf{0}$, is added. Furthermore, the following inequality is satisfied.

$$\max_{\mathbf{F}^H \mathbf{y} = \mathbf{0}} \frac{\mathbf{y}^H \mathbf{G}_{11} \mathbf{y}}{\mathbf{y}^H \mathbf{y}} \geq \max_{\bar{\mathbf{V}}_j^H \mathbf{y} = \mathbf{0}} \frac{\mathbf{y}^H \mathbf{G}_{11} \mathbf{y}}{\mathbf{y}^H \mathbf{y}}, \tag{A·10}$$

where $\mathbf{F}$ is an arbitrary matrix of dimension $(N-L) \times j$ and $\bar{\mathbf{V}}_j = \left(\bar{\mathbf{v}}_1\ \bar{\mathbf{v}}_2\ \cdots\ \bar{\mathbf{v}}_j\right)$. Finally, we have

$$\begin{aligned} \lambda_{j+1} &= \max_{\mathbf{V}_j^H \mathbf{x} = \mathbf{0}} \frac{\mathbf{x}^H \mathbf{G} \mathbf{x}}{\mathbf{x}^H \mathbf{x}} \geq \max_{\mathbf{V}_j^{(u)H} \mathbf{y} = \mathbf{0}} \frac{\mathbf{y}^H \mathbf{G}_{11} \mathbf{y}}{\mathbf{y}^H \mathbf{y}} \\ &\geq \max_{\bar{\mathbf{V}}_j^H \mathbf{y} = \mathbf{0}} \frac{\mathbf{y}^H \mathbf{G}_{11} \mathbf{y}}{\mathbf{y}^H \mathbf{y}} = \max_{\bar{\mathbf{V}}_j^H \mathbf{y} = \mathbf{0}} \frac{\mathbf{y}^H \left(\sum_{k=1}^{N-L} \bar{\lambda}_k \bar{\mathbf{v}}_k^H \bar{\mathbf{v}}_k^H \right) \mathbf{y}}{\mathbf{y}^H \mathbf{y}} \\ &= \bar{\lambda}_{j+1} = a_{j+1} \lambda_{j+1}. \end{aligned} \tag{A·11}$$

Since the eigenvalue of the correlation matrix is nonnegative, the region of the eigenvalue decay factor corresponding to the i-th eigenvalue, a_i, is given as

$$0 \leq a_i \leq 1. \tag{A·12}$$

Riichi Kudo received the B.S. and M.S. degrees in geophysics from Tohoku University, Japan, in 2001 and 2003, respectively. In 2003, he joined NTT Network Innovation Laboratories, Yokosuka, Japan. He has been researching in the MIMO communication systems and the beamforming method. He received the Young Engineer Award from the Institute of Electronics, Information and Communication Engineers (IEICE) Japan in 2006. His current research interests include multiuser MIMO communication systems and digital signal processing for optical coherent communication systems. He is a member of IEEE.

Yasushi Takatori was received his B.E. degree in electrical and communication engineering and his M.E. degree in system information engineering from Tohoku University, Sendai, Japan in 1993 and 1995, respectively. In 1995, he joined NTT Wireless Systems Laboratories, Nippon Telegraph and Telephone Corporation (NTT), in Japan. He is now working for NTT Network Innovation Laboratories. He was a visiting researcher at the Center for TeleInFrastructure (CTIF), Aalborg University, Aalborg, Denmark from 2004 to 2005. He received the Young Engineers Award from the IEICE of Japan in 2000, the Excellent Paper Award of WPMC in 2004 and YRP Award in 2005. His current research interests include smart antennas, multiuser MIMO systems, and spatial signal processing techniques. He is an associate editor of Springer Journal of Wireless Personal Communications. He is a member of the IEEE.

Kentaro Nishimori was born in Wakayama, Japan, in 1971. He received the B.E., M.E. and Dr.Eng. degrees in electrical and computer engineering from Nagoya Institute of Technology, Nagoya, Japan in 1994, 1996 and 2002, respectively. In 1996, he joined the NTT Wireless Systems Laboratories, Nippon Telegraph and Telephone Corporation (NTT), in Japan. He was a research engineer in NTT Network Innovation Laboratories. He is now a visiting researcher at the Center for Teleinfrastructure (CTIF), Aalborg University, Aalborg, Denmark (from 2006). He received the Young Engineers Award from the IEICE of Japan in 2001 and Young Engineer Award from IEEE AP-S Japan Chapter in 2001. His current research interests are Multi-user MIMO systems and cognitive radio systems. He is a member of IEEE.

Atsushi Ohta received the B.S. and M.S. degrees in Physics from Chiba University, Chiba, Japan, in 1988 and 1990, respectively. He joined NTT in 1990 and engaged in the development of multi-beam satellite communication systems. From 1997 to 2002, he engaged in the development of broadband wireless LAN system, named AWA (Advanced Wireless Access) and based on European standard, HiperLAN/2. He is currently researching and developing multiuser MIMO communication systems that offer improved utilization efficiency of radio frequency resources in the Access Network Service Systems Laboratories, NTT.

Shuji Kubota received the B.E. degree from the University of Electro-Communications, Tokyo in 1980 and the Ph.D. degree in Engineering from Osaka University in 1995. Since joining NTT in 1980, he has been engaged in the research and development of satellite communication systems, personal communication systems (PHS), software defined radio systems, wireless LAN systems, wireless access systems and wide-area sensor network systems. From 1991 to 1992, he was with the University of California, Davis as a visiting researcher. In 2008, he moved to Shibaura Institute of Technology, and he is currently a professor in the Department of Electrical Communications, College of Engineering, at Shibaura Institute of Technology, Tokyo. He is a member of IEEE.

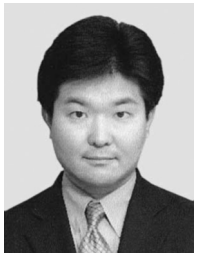

Masato Mizoguchi was born in Tokyo, Japan, in 1965. He received the B.E. and M.E. degrees in electrical engineering from Tokyo University of Science, Japan in 1989 and 1991, respectively. In 1991, he joined Nippon Telegraph and Telephone Corporation (NTT) and was mainly engaged in research and development of personal communication systems and high data rate wireless LANs including the IEEE 802.11a systems. He is currently a Senior Research Engineer, Supervisor in the Wireless Systems Innovation Laboratory of NTT Network Innovation Laboratories, where he is engaged in on future wireless broadband and ubiquitous systems. He received the Young Researcher's Award in 1998, the Best Paper Award in 2000 and the Achievement Award in 2006 from IEICE. He is a member of IEEE.